JOURNAL OF APPLIED ELECTROCHEMISTRY 17 (1987) 33–48

Kinetics and mechanism of anodic oxidation of chlorate ion to perchlorate ion on lead dioxide electrodes

N. MUNICHANDRAIAH, S. SATHYANARAYANA

Department of Inorganic and Physical Chemistry, Indian Institute of Science, Bangalore 560 012, India

Received 30 January 1986

The kinetics and mechanism of anodic oxidation of chlorate ion to perchlorate ion on titanium-substrate lead dioxide electrodes have been investigated experimentally and theoretically. It has been demonstrated that the ionic strength of the solution has a marked effect on the rate of perchlorate formation, whereas the pH of the solution does not influence the reaction rate. Experimental data have also been obtained on the dependence of the reaction rate on the concentration of chlorate ion in the solution at constant ionic strength. With these data, diagnostic kinetic criteria have been deduced and compared with corresponding quantities predicted for various possible mechanisms including double layer effects on electrode kinetics. It has thus been shown that the most probable mechanisms for anodic chlorate oxidation on lead dioxide anodes involve the discharge of a water molecule in a one-electron transfer step to give an adsorbed hydroxyl radical as the rate-determining step for the overall reaction.

Nomenclature

β	anodic energy transfer coefficient
ϕ_2	potential of outer Helmholtz plane with respect to solution
ϕ_M	potential of metal with respect to solution
ε	dielectric constant of solution
ε_0	permittivity of free space
θ	faradaic efficiency for anodic chlorate oxidation
A	adsorbed intermediate in Reaction 2
B	bulk species in Reaction 2
c_A	concentration of A at outer Helmholtz plane
c_B	concentration of B at outer Helmholtz plane
c_B^0	concentration of B in bulk
$c^0_{ClO_3^-}$	concentration of ClO_3^- in bulk
$c^0_{ClO_4^-}$	concentration of ClO_4^- in bulk
E	electrode potential corrected for ohmic drop
E_a	electrode potential as measured against reference electrode
E_s^0	standard electrode potential of Reaction 2
E_z	potential of zero charge of the anode in test solution
F	Faraday constant
f	$F/(RT)$
I_t	current at anode
I_{OER}	current used for oxygen evolution reaction at anode
I	current used for chlorate oxidation $(= I_t - I_{OER})$ at anode
i_t	I_t/anode area
i_{OER}	I_{OER}/anode area
i	I/anode area
J	total concentration of (uni–univalent) electrolytes in solution
K_2	integral capacitance of compact part of double layer
K_s	standard rate constant for Reaction 2, corrected for double layer effects
n_s	number of electrons involved in Reaction 2
p	$\partial \ln(-i)/\partial \ln c^0_{ClO_3^-}$
q_M	charge density on metal surface

0021–891X/87 $03.00 + .12

Q_t	quantity of electricity passed in given time interval	s	$\partial \ln(-i)/\partial$ pH
Q_{OER}	quantity of electricity required for oxygen evolution reaction in given time interval	T	absolute temperature
		t	$\partial \ln(-i)/\partial E$
		u	$(\varepsilon\varepsilon_0 RT/2\pi)^{1/2}$
R_Ω	ohmic resistance between anode and Luggin tip	V	volume of gases evolved in given time interval
R	gas constant	V_H	volume of hydrogen evolved in given time interval
r	$\partial \ln(-i)/\partial \ln J$	Z_B	charge on species B

1. Introduction

The anodic oxidation of chlorate ion to perchlorate ion, namely

$$ClO_3^- + H_2O \longrightarrow ClO_4^- + 2H^+ + 2e \quad (1)$$

is of considerable importance technologically as well as from a scientific point of view. The scientific importance of the above reaction stems from the unique conditions under which it takes place, for example, the oxidation occurring at high positive potentials (1.5 to 2.5 V versus SCE) in spite of the possibility of anodic oxygen evolution, the oxidation occurring on an oxide covered (or oxide coated) surface and the oxidation probably passing through several intermediate steps since it involves a transfer of two electrons and two reactant species.

Table 1. Mechanisms proposed in the literature for electro-oxidation of chlorate ion to perchlorate ion

Mechanisms	*References*
$2ClO_3^- \longrightarrow 2(ClO_3)_{ad} + 2e$ $2(ClO_3)_{ad} + H_2O \longrightarrow ClO_4^- + ClO_2^- + 2H^+ + \frac{1}{2}O_2$ $ClO_2^- + \frac{1}{2}O_2 \longrightarrow ClO_3^-$	[1]
$H_2O \longrightarrow (O)_{ad} + 2H^+ + 2e$ $(O)_{ad} + ClO_3^- \longrightarrow ClO_4^-$	[2]
$2ClO_3^- \longrightarrow (Cl_2O_6)_{ad} + 2e$ $(Cl_2O_6)_{ad} + H_2O \longrightarrow 2H^+ + ClO_3^- + ClO_4^-$	[3]
$ClO_3^- \longrightarrow (ClO_3)_{ad} + e$ $OH^- \longrightarrow (OH)_{ad} + e$ $(ClO_3)_{ad} + (OH)_{ad} \longrightarrow HClO_4$	[4, 5]
$ClO_3^- \longrightarrow (ClO_3)_{ad} + e$ $(ClO_3)_{ad} + H_2O \longrightarrow HClO_4 + H^+ + e$	[6]
$H_2O \longrightarrow (OH)_{ad} + H^+ + e$ $(OH)_{ad} + ClO_3^- \longrightarrow ClO_4^- + H^+ + e$	[7]
$H_2O \longrightarrow (OH)_{ad} + H^+ + e$ $(OH)_{ad} \longrightarrow (O)_{ad} + H^+ + e$ $(O)_{ad} + ClO_3^- \longrightarrow ClO_4^-$	[8]
$ClO_3^- \longrightarrow (ClO_3)_{ad} + e$ $(ClO_3)_{ad} + H_2O \rightleftharpoons ClO_4^- + 2H^+ + e$ (or OH^-) (or $ClO_4^- + H^+ + e$)	[9]

2. Previous work

There is little information in the literature on the theoretical formulation and experimental verification of the kinetics and mechanism of Reaction 1. The few references which have a bearing on the mechanism of anodic chlorate oxidation on platinum or lead dioxide anodes are listed in Table 1 along with the proposed mechanisms. A study of the literature in Table 1 shows that most of the mechanisms suggested are simply speculative, being based on indirect data which do not exclude other possible mechanisms, on doubtful interpretation of data, or on inadequate experimental support.

Preliminary studies in this work showed that the anodic oxidation of chlorate to perchlorate is accelerated by an increase in the concentration of perchlorate even at a constant concentration of chlorate. This fact suggests the presence of a strong double layer effect on the electrode kinetics which has not been examined in the literature. It is the objective of the present investigation to provide a formal kinetic analysis of Reaction 1 for several possible mechanisms also incorporating the double layer effects, and to deduce diagnostic criteria and compare these with experimental results.

3. Possible mechanisms

Several pathways may be postulated involving the generation and interaction of adsorbed radicals such as $(ClO_3)_{ad}$, $(OH)_{ad}$ and $(O)_{ad}$ on the anode surface resulting in the overall electrode process (Reaction 1). A fairly exhaustive list of such mechanisms with a single rate-determining step in a sequence of consecutive steps leading to Reaction 1 may be set up as shown in Table 2.

4. Kinetic analysis

A general representation for a rate-determining step in Table 2 is

$$A + B \longrightarrow P + n_s e \tag{2}$$

where A may be an adsorbed intermediate and B may be a bulk species present at the interface.

Reaction 1 is known to be kinetically irreversible. Hence, taking into account possible double layer effects, the reaction current (i), which is equal to that of the rate-determining step, is given by*

$$i = -n_s F K_s c_A c_B \exp[\beta n_s f(E - E_s^0 - \phi_2)] \tag{3}$$

where the concentrations c_A and c_B are at the reaction zone which is at an average potential ϕ_2 with respect to the solution.

The concentration of the adsorbed intermediate (c_A) is obtained by considering the nature of the quasi-reversible step preceding or succeeding the rate-determining step. The concentration of the species from the bulk of the solution (c_B) is related to its bulk concentration as $c_B = c_B^0 \exp(-\phi_2 Z_B f)$, since any mass transfer limitation in the solution is absent (cf. Results section).

In the absence of specific adsorption, ϕ_2 is equal to the potential of the outer Helmholtz plane (OHP). Since a weak specific adsorption of ClO_4^- and ClO_3^- ions may occur, by analogy with mercury-solution interface [11] it may be assumed that ϕ_2 is the potential of the OHP in the present case, to a good approximation. Values for ϕ_2 may be calculated from double layer theory [12]

* Cathodic current is considered positive. Though this classical convention is different from IUPAC recommendations, it is still under use in the current literature and text books on electrochemistry (see, for example, [10]). The current for Reaction 2 is with a negative sign.

Table 2. Possible mechanisms for the anodic oxidation of chlorate ion to perchlorate ion in aqueous media[a]

Mechanism	*Mechanism steps*
I	$ClO_3^- + H_2O \longrightarrow ClO_4^- + 2H^+ + 2e$
II	$ClO_3^- + OH^- \longrightarrow ClO_4^- + H^+ + 2e$
III	$ClO_3^- \longrightarrow (ClO_3)_{ad} + e$ $(ClO_3)_{ad} + H_2O \rightleftharpoons ClO_4^- + 2H^+ + e$
IV	$ClO_3^- \rightleftharpoons (ClO_3)_{ad} + e$ $(ClO_3)_{ad} + H_2O \longrightarrow ClO_4^- + 2H^+ + e$
V	$ClO_3^- \longrightarrow (ClO_3)_{ad} + e$ $(ClO_3)_{ad} + OH^- \rightleftharpoons ClO_4^- + H^+ + e$
VI	$ClO_3^- \rightleftharpoons (ClO_3)_{ad} + e$ $(ClO_3)_{ad} + OH^- \longrightarrow ClO_4^- + H^+ + e$
VII	$OH^- \longrightarrow (O)_{ad} + H^+ + 2e$ $ClO_3^- + (O)_{ad} \rightleftharpoons ClO_4^-$
VIII	$OH^- \rightleftharpoons (O)_{ad} + H^+ + 2e$ $ClO_3^- + (O)_{ad} \longrightarrow ClO_4^-$
IX	$H_2O \longrightarrow (O)_{ad} + 2H^+ + 2e$ $ClO_3^- + (O)_{ad} \rightleftharpoons ClO_4^-$
X	$H_2O \rightleftharpoons (O)_{ad} + 2H^+ + 2e$ $ClO_3^- + (O)_{ad} \longrightarrow ClO_4^-$
XI	$OH^- \longrightarrow (OH)_{ad} + e$ $ClO_3^- + (OH)_{ad} \rightleftharpoons ClO_4^- + H^+ + e$
XII	$OH^- \rightleftharpoons (OH)_{ad} + e$ $ClO_3^- + (OH)_{ad} \longrightarrow ClO_4^- + H^+ + e$
XIII	$H_2O \longrightarrow (OH)_{ad} + H^+ + e$ $ClO_3^- + (OH)_{ad} \rightleftharpoons ClO_4^- + H^+ + e$
XIV	$H_2O \rightleftharpoons (OH)_{ad} + H^+ + e$ $ClO_3^- + (OH)_{ad} \longrightarrow ClO_4^- + H^+ + e$
XV	$ClO_3^- \longrightarrow (ClO_3)_{ad} + e$ $OH^- \rightleftharpoons (OH)_{ad} + e$ $(ClO_3)_{ad} + (OH)_{ad} \rightleftharpoons ClO_4^- + H^+$
XVI	$ClO_3^- \rightleftharpoons (ClO_3)_{ad} + e$ $OH^- \longrightarrow (OH)_{ad} + e$ $(ClO_3)_{ad} + (OH)_{ad} \rightleftharpoons ClO_4^- + H^+$
XVII	$ClO_3^- \rightleftharpoons (ClO_3)_{ad} + e$ $OH^- \rightleftharpoons (OH)_{ad} + e$ $(ClO_3)_{ad} + (OH)_{ad} \longrightarrow ClO_4^- + H^+$
XVIII	$ClO_3^- \rightleftharpoons (ClO_3)_{ad} + e$ $H_2O \longrightarrow (OH)_{ad} + H^+ + e$ $(ClO_3)_{ad} + (OH)_{ad} \rightleftharpoons ClO_4^- + H^+$

[a] In the mechanisms listed, one arrow represents the rate-determining step while two arrows indicate kinetically reversible (i.e. fast) step.

through the equation for the charge density (q_M) on the metal surface:

$$q_M = \left(\frac{2\varepsilon\varepsilon_0 RTJ}{\pi}\right)^{1/2} \sinh\left(\frac{\phi_2 f}{2}\right) \tag{4}$$

where J is the sum of the concentrations of univalent electrolytes in solution ($NaClO_3$ and $NaClO_4$) in the present case.

Since the anode potential for the oxidation of chlorate to perchlorate at practical current densities (0.1 to 1.0 A cm^{-2}) on PbO_2 electrodes is in the range 1.5 to 2.5 V versus SCE, whereas the potential of zero charge of PbO_2 in neutral media (such as KNO_3) is about 0.8 V versus SCE [13], it follows that $\phi_2 f \gg 1$. Hence, from Equation 4

$$q_M \approx \left(\frac{\varepsilon\varepsilon_0 RTJ}{2\pi}\right)^{1/2} \exp\left(\frac{\phi_2 f}{2}\right) \tag{5}$$

Further, consistent with the assumption of weak or no specific adsorption,

$$q_M = K_2(\phi_M - \phi_2) \tag{6}$$

where K_2 is the integral capacitance of the compact part of the double layer.

On combining Equations 5 and 6 and noting that, in the present case

$$\ln [K_2(\phi_M - \phi_2)] = \ln [K_2(E - E_z - \phi_2)] \approx \ln [K_2(E - E_z)]$$

it follows that

$$\phi_2 \approx \frac{1}{f}[2 \ln (E - E_z) - \ln J + 2 \ln (K_2/u)] \tag{7}$$

On substituting into Equation 3 the above expression for ϕ_2, and appropriate expressions for c_A and c_B which depend on the mechanism chosen, the final current–potential relation may be derived as outlined in the Appendix for each mechanism listed in Table 2. As may be seen from the Appendix, the final rate equation for any mechanism considered is of the form

$$\ln (-i) = \text{constant} + p \ln c^0_{ClO_3^-} + r \ln J + s \text{ pH} + t E \tag{8}$$

On partial differentiation with respect to the chosen variables, the kinetic criteria for mechanism diagnosis, namely

Table 3. Diagnostic kinetic criteria for various mechanisms listed in Table 2

Mechanism	*Diagnostic kinetic criteria*			
	p	*r*	*s*	*t*
I	1	$-(1 - 2\beta)$	0	$2\beta f$
II	1	$-2(1 - \beta)$	2.3	$2\beta f$
III	1	$-(1 - \beta)$	0	βf
IV	1	β	0	$(1 + \beta)f$
V	1	$-(1 - \beta)$	0	βf
VI	1	$-(1 - \beta)$	2.3	$(1 + \beta)f$
VII	0	$-(1 - 2\beta)$	2.3	$2\beta f$
VIII	1	-1	4.6	$2f$
IX	0	2β	0	$2\beta f$
X	1	-1	4.6	$2f$
XI	0	$-(1 - \beta)$	2.3	βf
XII	1	$-(1 - \beta)$	2.3	$(1 + \beta)f$
XIII	0	β	0	βf
XIV	1	$-(1 - \beta)$	2.3	$(1 + \beta)f$
XV	1	$-(1 - \beta)$	0	βf
XVI	0	$-(1 - \beta)$	2.3	βf
XVII	1	0	2.3	$2f$
XVIII	0	β	0	βf

$$p = \frac{\partial \ln(-i)}{\partial \ln c^0_{ClO_3^-}}; \quad r = \frac{\partial \ln(-i)}{\partial \ln J}; \quad s = \frac{\partial \ln(-i)}{\partial \text{pH}}; \quad t = \frac{\partial \ln(-i)}{\partial E}$$

are readily derived.

The results thus obtained are summarized in Table 3, from which it may be seen that a majority of the mechanisms postulated are characterized by distinguishable kinetic criteria if suitable experimental data are available.

5. Experimental aspects

5.1. *Chemicals*

Reagent grade $NaClO_3$ and $NaClO_4$ were found to contain NaCl as an impurity which adversely affected the measurements as well as the stability of the PbO_2 anode. $NaClO_3$ was therefore purified by recrystallization twice from distilled water. $NaClO_4$ solution was purified by pre-electrolysis using PbO_2(Ti) anodes and stainless steel cathodes until the NaCl impurity was removed. The resulting solution was assayed for $NaClO_3$ and $NaClO_4$ and used accordingly to prepare solutions of required composition.

5.2. *Electrodes*

High surface area β-PbO_2(Ti) anodes were prepared as reported before [14]. Cathodes were 316-grade stainless steel sheets. The reference electrode was a calomel electrode saturated with NaCl as the electrolyte (SSCE) in order to eliminate plugging of capillary junctions in the reference electrode path by the slightly soluble $KClO_4$, which would form if KCl were used as the electrolyte.

5.3. *Solutions*

In order to obtain diagnostic kinetic criteria to identify the mechanisms of Reaction 1 with respect to each concentration variable while keeping other items constant, experiments were carried out with solutions of ($NaClO_3$ + $NaClO_4$) of different ionic strengths, each ionic strength being achieved with different proportions of $NaClO_3$ and $NaClO_4$. The pH of the solutions was measured using a calibrated pH meter correct to ± 0.1 pH. Adjustment of the pH of the test solution was effected by adding dilute $HClO_4$ or dilute NaOH solution.

5.4. *Cell*

The electrochemical cell consisted of a glass vessel sized to hold about 0.6 litres of solution to a height of about 30 cm above the electrodes, the solution being kept well stirred with a Teflon-coated magnetic stirrer. These design factors proved successful in holding the pH of the solution automatically constant during the electrolysis within ± 0.2 unit of the initial value, due to an efficient mixing of anolyte and catholyte streams. The working electrode and the counter electrodes had an integral stem of the respective metals, the upper ends of which were connected through titanium screw terminals to titanium rods projecting out of the cell through appropriate leak-proof holes in a Teflon stopper. The reference electrode was connected to the cell through an all-glass 'salt bridge' having a closed ungreased stopcock, the two sides of which were filled with the respective salt solutions (NaCl on the reference electrode side; test solution on the other side). The salt bridge terminated in a Luggin tip aligned close to the centre of the working electrode. The Luggin tip was loosely plugged with a piece of cleaned nylon cloth to prevent entry of gas bubbles into the salt bridge vitiating the potential measurements. The mixture of electrolytic gases (H_2, O_2, water vapour) was

led out of the cell into an all-glass Orsat-type gas analysis unit through a short length of polyethylene tubing. The temperature of the cell was maintained at 60 ± 2° C by means of a thermostatically controlled water jacket.

5.5. *Analytical aspects*

NaCl in $NaClO_3$ or $NaClO_4$ solution, if present, was estimated by potentiometric titration against standard silver nitrate solution using pure silver wire as the indicator electrode. In this case, the SSCE reference electrode was separated from the test solution by a salt bridge of $NaNO_3$ immobilized in agar gel to prevent interaction of the test solution with the solution in the reference electrode. The electromotive force of the cell was measured with an electrometric voltmeter (input impedance $> 10^{15}\,\Omega$), resulting in a titration accuracy of ±2% when the concentration of NaCl in the test solution was 0.1 mM.

$NaClO_3$ was estimated by the standard procedure [15] of reduction with excess ferrous ammonium sulphate in acid medium and back titration of unreacted ferrous salt against a standard dichromate solution using sodium diphenylamine sulphonate as the indicator. The procedure was standardized with recrystallized $KClO_3$ and the accuracy of determination was ±2% for a concentration level of $30\,g\,l^{-1}$ $KClO_3$.

$NaClO_4$ was estimated by first determining the total cation concentration of the mixture and then subtracting the concentrations of $NaClO_3$ and NaCl as determined above. The total cation concentration was estimated [16] by passing the test solution through a column containing a cation exchange resin and titrating the acid produced in the effluent against standard NaOH solution. The accuracy of determination of $NaClO_4$ was found to be ±5%.

Oxygen and hydrogen in the electrolytic gases were estimated by collecting the gases for a definite duration of electrolysis at constant current in the Orsat apparatus, measuring the volume (v) of the gas mixture using a water manometer, then absorbing the oxygen in a freshly prepared alkaline pyrogallol solution and measuring the residual volume (v_H) of the hydrogen gas with a water manometer. Volume corrections due to the prevailing barometric pressure and room temperature, and pressure corrections due to the vapour pressure of water were applied to estimate the amount of H_2 present at STP. The amount of oxygen at STP in the original gas sample was estimated by difference ($v - v_H$) with due corrections for barometric pressure and ambient temperature. Precautions were taken to flush out completely the air initially present in the Orsat apparatus by the electrolytic gases, before collecting the gas sample for analysis.

The apparatus was calibrated by electrolysing pure NaOH (20%) solution between nickel electrodes in the same cell. The procedure adopted was confirmed to yield an accuracy of ±1% for the determination of hydrogen and oxygen in the gas mixture.

With the above set-up, it was established that cathodic hydrogen evolution occurred at 100% current efficiency during the electrolysis of $NaClO_3$ + $NaClO_4$ solutions. In other words, the cathodic reduction of perchlorate to chlorate, or of chlorate to chloride does not take place to any significant extent. The assay of the solution before and after electrolysis for chloride, chlorate and perchlorate confirmed these conclusions.

5.6. *Anode efficiency*

The faradaic efficiency for anodic oxidation of chlorate to perchlorate was obtained by the gas analysis data as $(Q_t - Q_{OER})/Q_t$, where Q_{OER} is the quantity of electricity required for the oxygen evolved and Q_t is the total quantity of electricity passed during the interval of collecting the gas for analysis. The efficiency data were thus obtained, point by point, at various cell currents on each polarization curve.

5.7. *Electrical circuit*

Electrochemical measurements were carried out in the galvanostatic mode using a regulated power supply and an adjustable high resistance in series with the cell. Further, a silicon diode with low reverse-current characteristic was used in series with the cell to prevent any cathodic polarization of the PbO_2 working electrode inadvertently or during a mains power failure etc. All the measuring instruments were calibrated before the experiments.

The galvanostatic steady-state anodic polarization curves were recorded point by point, a steady state being deemed to have been attained when the fluctuation in the anode potential at any given current decreased to less than $1.0\,mV\,min^{-1}$. This usually required about 2–5 min at each current. Each polarization curve was recorded in increasing as well as decreasing direction of polarization from the open-circuit potential, and both before and after the measurement of faradaic efficiency at various currents. The final polarization curve was thus arrived at as an average of four sets of data points at each cell current.

5.8. *Correction of polarization curves for simultaneous oxygen evolution reaction*

Anode polarization curves were obtained by plotting the anode potential against the current density corrected for the oxygen evolution reaction ($i = i_t - i_{OER} = i_t\theta$, where θ is the current efficiency for anodic perchlorate formation at the anode current density, i_t).

6. Results and discussion

6.1. *Polarization curves*

The anodic galvanostatic (steady state) polarization curves for $NaClO_3 + NaClO_4$ solutions with different concentration ratios were all found to merge into a narrow band resulting in a single average polarization curve as shown in Fig. 1. The effect of stirring the solution at different rates is shown in Fig. 2.

It may be seen from Figs 1 and 2 that the polarization curve shows a continuous change without a well-defined Tafel line even though the overpotentials are large compared to RT/F and mass transfer control is absent. This apparent nonlinear Tafel behaviour may be due to an ohmic drop

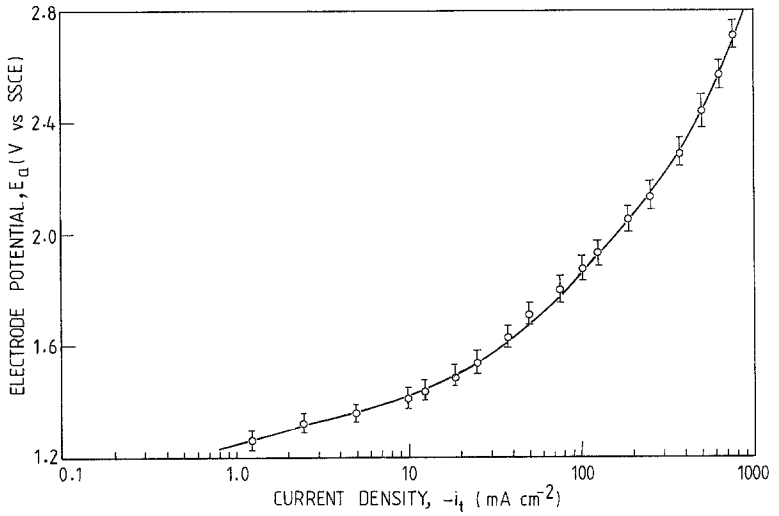

Fig. 1. Steady state anodic galvanostatic polarization curve for β-PbO_2(Ti) electrode in contact with mixed electrolyte solutions of $NaClO_3 + NaClO_4$ at 60 ± 2° C and pH 6.5 ± 0.2. The vertical spread shows the range of values observed for mixed solutions of ten different concentrations (M) of $NaClO_3 + NaClO_4$, namely: 2 + 0, 2 + 1, 2 + 2, 2 + 3, 2 + 4, 3 + 3, 4 + 1, 4 + 2, 4 + 3, and 5 + 1.

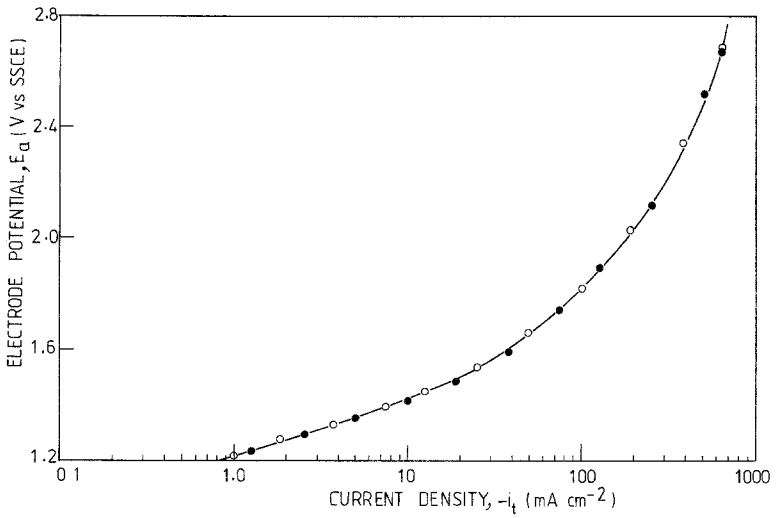

Fig. 2. Steady state anodic galvanostatic polarization curve for β-PbO_2(Ti) electrode in contact with $NaClO_3$ (4 M) + $NaClO_4$ (1 M) solution at 60 ± 2° C and pH 6.5 ± 0.2, at different rates of rotation of the stirrer: ○, 1200 r.p.m.; ●, 2600 r.p.m.

in the measured anode potential and due to the current for the side reaction (simultaneous oxygen evolution reaction) in the measured current.

6.2. *Current efficiency*

The current (or faradaic) efficiency curves for anodic perchlorate formation are shown in Fig. 3.

It may be seen from Fig. 3 that the current efficiency for anodic oxidation of chlorate increases not only with increase in the current density as noted in the earlier literature [9], but also with increase in the ionic strength of the solution at constant chlorate concentration, which is a fact of considerable importance in the elucidation of the mechanism.

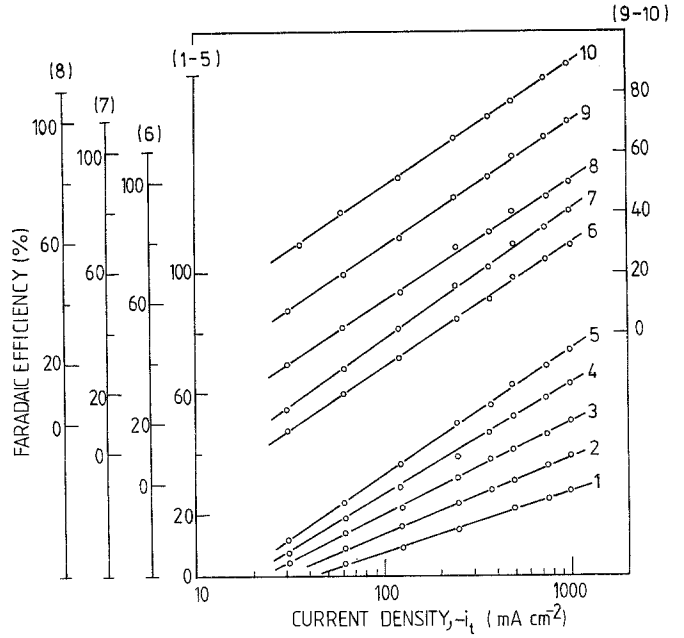

Fig. 3. Faradaic efficiency for anodic chlorate oxidation on β-PbO_2(Ti) electrode as a function of current density in the mixed electrolyte solutions of different concentrations of $NaClO_3$ + $NaClO_4$, namely: 1, 2 + 0; 2, 2 + 1; 3, 2 + 2; 4, 2 + 3; 5, 2 + 4; 6, 3 + 3; 7, 4 + 2; 8, 5 + 1; 9, 4 + 1; 10, 4 + 3; at 60 ± 2° C and pH 6.5 ± 0.2. Different scales of y-axis correspond to curve numbers shown in parenthesis.

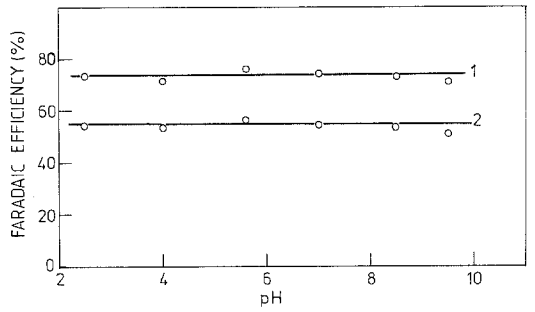

Fig. 4. Faradaic efficiency of anodic chlorate oxidation on β-PbO_2(Ti) electrode at 60 $\pm$ 2° C, as a function of pH of the solution of $NaClO_3$(5 M) + $NaClO_4$(1 M) at anode potentials of: 1, 2.50 V; 2, 2.00 V versus SSCE.

6.3. *Effect of pH*

The dependence of the anode efficiency for chlorate oxidation on the bulk pH of the solution is shown in Fig. 4 at two typical anode potentials. Anode potentials rather than currents were controlled here since the diagnostic kinetic criteria required in the case of pH as the controlled variable is $(\partial \ln(-i)/\partial \text{pH})$ at constant value of E, $c^0_{ClO_3^-}$ and $c^0_{ClO_4^-}$.

It may be inferred from Fig. 4 that the current efficiency for perchlorate formation on PbO_2 anode is independent of the pH of the solution. Therefore, it follows that

$$s = \frac{\partial \ln(-i)}{\partial \text{pH}} = 0 \tag{9}$$

6.4. *Corrected polarization curves*

From Figs 1 and 3, the total current at each anode potential may be corrected for the current used in the oxygen evolution reaction. The resulting partial polarization curves for anodic chlorate oxidation to perchlorate alone are shown in Fig. 5.

It may be seen from Fig. 5 that the polarization curves corrected for the oxygen current show a nonlinear Tafel behaviour which may be attributed to uncompensated ohmic drops in the measured potential. The uncompensated ohmic resistance (R_Ω) may be estimated [17] from the slope of $dE_a/d\ln(-I)$ versus $(-I)\, dI_t/dI$ curve to a good approximation since, at constant R_Ω, the rate

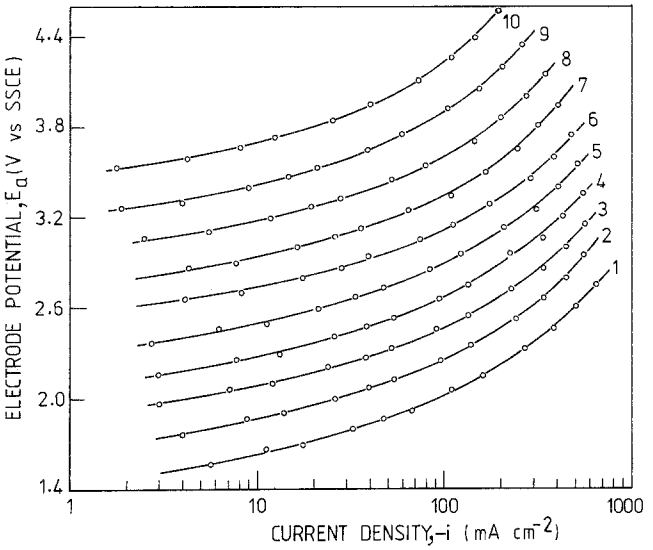

Fig. 5. Potential of β-PbO_2(Ti) electrode as a function of current density used for oxidizing chlorate to perchlorate only, at 60 $\pm$ 2° C, pH 6.5 $\pm$ 0.2. Mixed electrolyte solutions used have different concentrations (M) of $NaClO_3$ + $NaClO_4$, namely: 1, 4 + 3; 2, 5 + 1; 3, 4 + 2; 4, 3 + 3; 5, 2 + 4; 6, 4 + 1; 7, 2 + 3; 8, 2 + 2; 9, 2 + 1, 10, 2 + 0. Curve 2 is shifted vertically up by 0.2 V from curve 1, curve 3 by 0.4 V, and so on until curve 10 by 1.8 V.

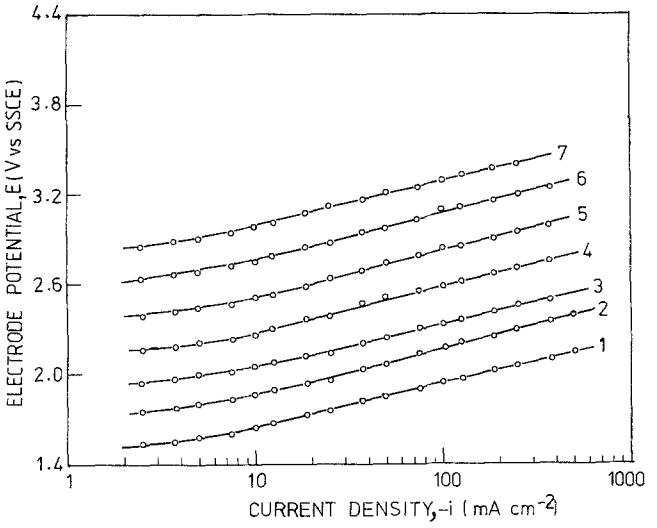

Fig. 6. Polarization curves (potentials corrected for ohmic drop) for anodic oxidation of chlorate to perchlorate on β-PbO_2(Ti) electrode at 60 ± 2° C, pH 6.5 ± 0.2 in the mixed electrolyte solutions of different concentrations (M) of $NaClO_3$ + $NaClO_4$, namely: 1, 5 + 1; 2, 4 + 2; 3, 3 + 3; 4, 2 + 4; 5, 2 + 3; 6, 2 + 2; 7, 2 + 1. Curve 2 is shifted vertically up by 0.2 V from curve 1, curve 3 by 0.4, and so on until curve 7 by 1.2 V.

equation in the Tafel region can be written as

$$E_a + I_t R_\Omega = \frac{1}{\beta f} \ln I + \text{constant}$$

With the value of R_Ω found thus ($\sim 0.1\ \Omega$), the measured anode potential (E_a) may be corrected for the ohmic drop ($-I_t R_\Omega$) at each anode current ($-I_t$) resulting in the true anode polarization curves shown in Fig. 6.

It may be seen from Fig. 6 that the corrected polarization curves show good Tafel lines of nearly the same slope for all the solutions studied. The average Tafel slope is found to be 0.30 ± 0.02 V.

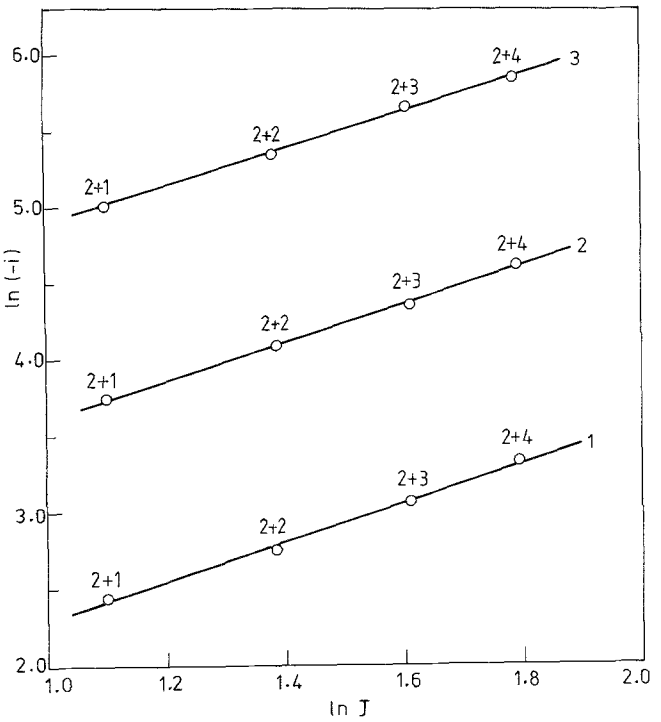

Fig. 7. Plot of ln $(-i)$ versus ln J at constant values of chlorate concentration, pH 6.5 ± 0.2 and anode potentials, E, of: 1, 1.8 V; 2, 2.0 V; 3, 2.2 V versus SSCE. The concentrations (M) of $NaClO_3$ + $NaClO_4$ solution are shown above the experimental points.

From this value of the Tafel slope, it follows that

$$t = \frac{\partial \ln (-i)}{\partial E} = 7.7 \pm 0.5\,\mathrm{V}^{-1} \tag{10}$$

The parameters p and r may also be evaluated from the corrected polarization curves in Fig. 6 as follows. At any given potential, E, currents are read from Fig. 6 corresponding to (a) solutions with constant ionic strength and variable $c^0_{ClO_3^-}$, and (b) solutions with constant $c^0_{ClO_3^-}$ and variable ionic strength. Experimental curves are thus derived showing the dependence of $\ln(-i)$ versus $\ln J$ at constant $c^0_{ClO_3^-}$ for chosen values of E, as well as the dependence of $\ln(-i)$ versus $\ln c^0_{ClO_3^-}$ at constant J for chosen values of E. The results are shown in Figs 7 and 8.

From the slopes of the curves in these figures, the average values of p and r are obtained. Thus

$$p = \frac{\partial \ln (-i)}{\partial \ln c^0_{ClO_3^-}} = 0.12 \pm 0.02 \tag{11}$$

and

$$r = \frac{\partial \ln (-i)}{\partial \ln J} = 1.25 \pm 0.02 \tag{12}$$

6.5. *Comparison of theory with experiment*

The diagnostic kinetic parameters p, r, s and t obtained from experiment (Equations 9–12) may now be compared with the values predicted from Table 3, assuming that β is equal to 0.5, a probable value for an elementary step of electron transfer. It is thus found, surprisingly, that only two of the eighteen mechanisms listed in Table 2, namely mechanisms XIII and XVIII, show an acceptable fit with experimental data. The corresponding values are shown in Table 4. All other mechanisms in

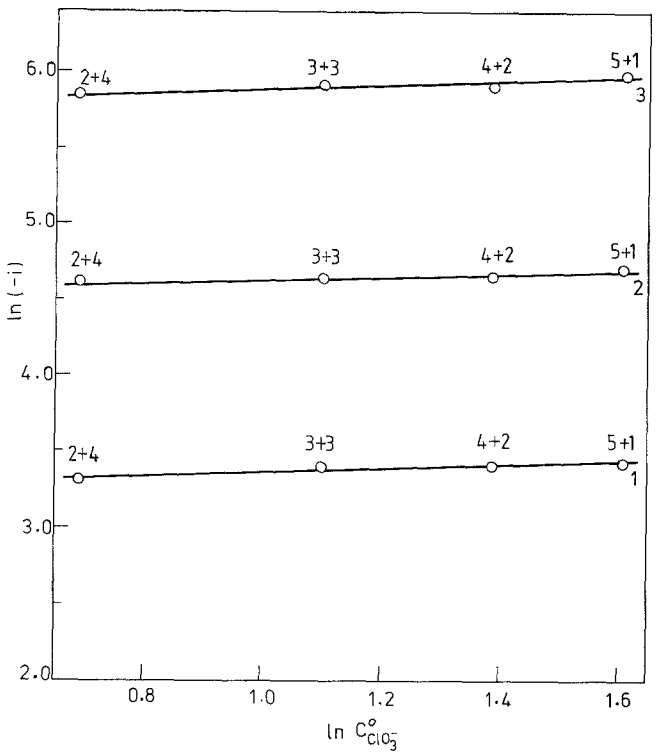

Fig. 8. Plot of $\ln(-i)$ versus $\ln c^0_{ClO_3^-}$ at constant values of total salt concentration, pH 6.5 ± 0.2 and anode potentials, E, of: 1, 1.8 V; 2, 2.0 V; 3, 2.2 V versus SSCE. The concentrations (M) of $NaClO_3$ + $NaClO_4$ solution are shown above the experimental points.

Table 4. Comparison of experimental and theoretical values

Kinetic parameter	*Experimental value of parameter*	*Theoretical value of parameter for mechanism XIII or XVIII*
p	0.12	0
r	1.25	0.5
s	0	0
t (V^{-1})	7.7	20

Table 2 show a substantially poorer fit with experiment. Mechanisms XIII and XVIII are therefore the preferred mechanisms. It is not possible, however, to discriminate further between them at this stage.

It thus follows from the above study of electrode kinetics that the mechanism of anodic oxidation of chlorate to perchlorate on β–PbO_2(Ti) anodes involves the anodic oxidation of water in a one-electron transfer step to give an adsorbed (OH) radical as the rate-determining step. Perchlorate ion is produced by a subsequent fast oxidation step involving either the chlorate ion or an adsorbed chlorate radical and the adsorbed (OH) radical. Schematically, this may be illustrated as follows:

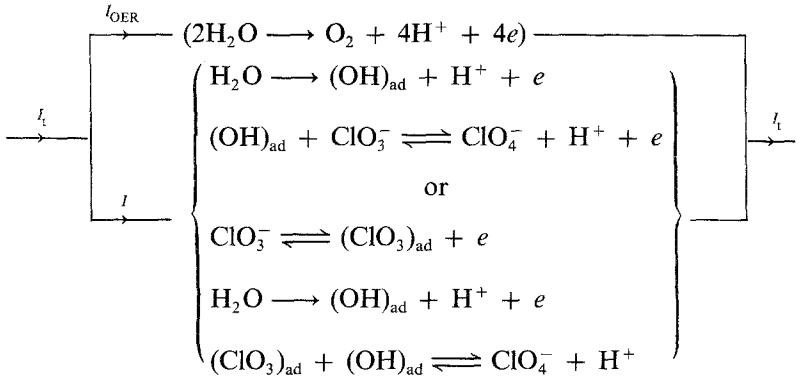

7. Conclusions

A variety of mechanisms may be proposed for the anodic oxidation of chlorate ion to perchlorate ion. Determination of electrochemical reaction orders, double layer effects and Tafel slopes of polarization curves, corrected for the current due to anodic oxygen evolution, on titanium-substrate lead dioxide anodes leads to the conclusion that the most probable mechanism involves the formation of an adsorbed hydroxyl radical from the oxidation of water as the rate-determining step for the overall reaction.

Acknowledgement

Financial support for this work by ISRO through a RESPOND project is gratefully acknowledged.

Appendix

Derivation of current–potential relations and kinetic criteria for the mechanisms listed in Table 2.

Mechanism I. In Equation 2, 'A' is absent while 'B' denotes ClO_3^- or H_2O (i.e. both non-adsorbed species). Hence

$$(-i) = 2FK_s c^0_{ClO_3^-} \exp(f\phi_2) c^0_{H_2O} \exp[2\beta f((E - E^0_s - \phi_2)]$$

On substituting for ϕ_2 from Equation 7 and simplifying,

$$\ln(-i) = \text{const} + \ln c^0_{ClO_3^-} - (1 - 2\beta) \ln J + 2(1 - 2\beta) \ln(E - E_z) + 2\beta fE$$

On partial differentiation

$$t = \frac{\partial \ln(-i)}{\partial E} = 2\beta f + \frac{2(1 - 2\beta)}{E - E_z}$$

Considering the orders of magnitude involved ($\beta \sim 0.5$; $(E - E_z) \sim 1$ to 2 V; $f \sim 40\,V^{-1}$) it follows that $[(1 - 2\beta)/(E - E_z)] \ll \beta f$. Hence $t \approx 2\beta f$. Further,

$$p = \frac{\partial \ln(-i)}{\partial \ln c^0_{ClO_3^-}} = 1$$

$$r = \frac{\partial \ln(-i)}{\partial \ln J} = -(1 - 2\beta)$$

$$s = \frac{\partial \ln(-i)}{\partial \text{pH}} = 0$$

Mechanism II. Similar to Mechanism I except that instead of c_{H_2O}, one has here $c_{OH^-} = c^0_{OH^-} \exp(f\phi_2)$. Finally

$$\ln(-i) = \text{const} + \ln c^0_{ClO_3^-} + \ln c^0_{OH^-} - 2(1 - \beta) \ln J + 4(1 - \beta) \ln(E - E_z) + 2\beta fE$$

Hence $p = 1$; $r = -2(1 - \beta)$; $s = 2.3$; and $t \approx 2\beta f$ (cf. Mechanism I).

Mechanism III. Similar to Mechanism I. Finally

$$\ln(-i) = \text{const} + \ln c^0_{ClO_3^-} - (1 - \beta) \ln J + 2(1 - \beta) \ln(E - E_z) + \beta fE$$

Hence $p = 1$; $r = -(1 - \beta)$; $s = 0$; and $t \approx \beta f$ (cf. Mechanism I).

Mechanism IV. In Equation 2, 'A' is the $(ClO_3)_{ad}$ radical, and 'B' is H_2O. The concentration of $(ClO_3)_{ad}$ is obtained through the Nernst equation applied to the quasi-reversible step preceding the rate-determining step. Thus

$$\ln c_{(ClO_3)_{ad}} = \ln c^0_{ClO_3^-} + f(E - E^0)$$

where E^0 is the standard electrode potential of the quasi-reversible step. Finally

$$\ln(-i) = \text{const} + \ln c^0_{ClO_3^-} + \beta \ln J - 2\beta \ln(E - E_z) + (1 + \beta) fE$$

Therefore $p = 1$; $r = \beta$; $s = 0$; and $t \approx (1 + \beta) f$ (cf. Mechanism I).

Mechanism V. Analysis identical to Mechanism III.

Mechanism VI. Analysis similar to Mechanism IV except that 'B' is OH^- and $c_{OH^-} = c^0_{OH^-} \exp(f\phi_2)$. Finally

$$\ln(-i) = \text{const} + \ln c^0_{ClO_3^-} + \ln c^0_{OH^-} (1-\beta) \ln J + 2(1-\beta) \ln (E - E_z) + (1+\beta) fE$$

Therefore $p = 1$; $r = -(1-\beta)$; $s = 0$; and $t \approx (1+\beta)f$ (cf. Mechanism I).

Mechanism VII. There is only one reactant OH^- in the rate-determining step.

$$\ln(-i) = \text{const} + \ln c^0_{OH^-} - (1-2\beta) \ln J + 2(1-2\beta) \ln (E - E_z) + 2\beta fE$$

Hence $p = 0$; $r = -(1-2\beta)$; $s = 2.3$; and $t \approx 2\beta f$ (cf. Mechanism I).

Mechanism VIII. The rate-determining step does not involve charge transfer. 'A' is the $(0)_{ad}$ radical, and 'B' is ClO_3^- in Equation 2. c_A is obtained as in Mechanism IV. Finally

$$\ln(-i) = \text{const} + \ln c^0_{ClO_3^-} - \ln c^0_{OH^-} + \ln c^0_{H^+} - \ln J + 2 \ln (E - E_z) + 2fE$$

Hence $p = 1$; $r = -1$; $s = 4.6$; and $t \approx 2f$ (cf. Mechanism I).

The following results for the remaining mechanisms are obtained by an analysis similar to the above cases.

Mechanism IX.

$$\ln(-i) = \text{const} + 2\beta \ln J - 4\beta \ln (E - E_z) + 2\beta fE$$

Hence $p = 0$; $r = 2\beta$; $s = 0$; and $t \approx 2\beta f$.

Mechanism X.

$$\ln(-i) = \text{const} + \ln c^0_{ClO_3^-} 2 \ln c^0_{H^+} - \ln J + 2 \ln (E - E_z) + 2fE$$

Hence $p = 1$; $r = -1$; $s = 4.6$; and $t \approx 2f$.

Mechanism XI.

$$\ln(-i) = \text{const} + \ln c^0_{OH^-} + 2(1-\beta) \ln (E - E_z) - (1-\beta) \ln J + \beta fE$$

Hence $p = 0$; $r = -(1-\beta)$; $s = 2.3$; and $t \approx \beta f$.

Mechanism XII.

$$\ln(-i) = \text{const} + \ln c^0_{ClO_3^-} + \ln c^0_{OH^-} - (1-\beta) \ln J + 2(1-\beta) \ln (E - E_z) + (1+\beta) fE$$

Hence $p = 1$; $r = -(1-\beta)$; $s = 2.3$; and $t \approx (1+\beta)f$.

Mechanism XIII.

$$\ln(-i) = \text{const} + \beta \ln J - 2\beta \ln (E - E_z) + \beta fE$$

Hence $p = 0$; $r = \beta$; $s = 0$; and $t \approx \beta f$.

Mechanism XIV.

$$\ln(-i) = \text{const} + \ln c^0_{ClO_3^-} - \ln c^0_{H^+} - (1-\beta) \ln J + 2(1-\beta) \ln (E - E_z) + (1+\beta) fE$$

Hence $p = 1$; $r = -(1-\beta)$; $s = 2.3$; and $t \approx (1+\beta)f$.

Mechanism XV. Results are identical to Mechanism III.

Mechanism XVI. Results are identical to Mechanism XI.

Mechanism XVII. Double layer effects are absent since both reactants in the rate-determining step are adsorbed intermediates.

$$\ln(-i) = \text{const} + \ln c^0_{ClO_3^-} + \ln c^0_{OH^-} + 2fE$$

Hence $p = 1$; $r = 0$; $s = 2.3$; and $t \approx 2f$.

Mechanism XVIII. Results identical to Mechanism XIII.

References

[1] W. Oechsli, *Z. Elekrochem.* **9** (1903) 807.
[2] C. W. Bennett and E. L. Mack, *Trans. Electrochem. Soc.* **29** (1916) 323.
[3] N. V. S. Knibbs and H. Palfreeman, *Trans. Faraday Soc.* **16** (1920) 402.
[4] K. Sugino and S. Aoyagi, *J. Electrochem. Soc.* **103** (1956) 166.
[5] T. Osuga, S. Fujii, K. Sugino and T. Sekine, *ibid.* **116** (1969) 203.
[6] K. C. Narasimham, S. Sundararajan and H. V. K. Udupa, *ibid.* **108** (1961) 798.
[7] Yung-Chao Chu and Shih-Hsiung Chin, *Chem. Abs.* **67** (1967) 7479e.
[8] M. P. Grotheer and E. H. Cook, *Electrochem. Technol.* **6** (1968) 221.
[9] O. de Nora, P. Gallone, C. Traini and G. Meneghini, *J. Electrochem. Soc.* **116** (1969) 146.
[10] A. J. Bard and L. R. Faulkner, 'Electrochemical Methods: Fundamentals and Applications', John Wiley, New York (1980) p. 28.
[11] H. Wroblawa, Z. Kovac and J. O'M. Bockris, *Trans. Faraday Soc.* **61** (1965) 1523.
[12] P. Delahay, 'Double Layer and Electrode Kinetics', Interscience Publishers, New York (1965).
[13] J. P. Carr, N. A. Hampson and R. Taylor, *J. Electroanal. Chem.* **27** (1970) 109.
[14] N. Munichandraiah and S. Sathyanarayana, *J. Appl. Electrochem.* **17** (1987) 22.
[15] A. I. Vogel, 'A Text Book of Quantitative Inorganic Analysis', 3rd edn, The English Language Book Society and Longmans Green & Co. Ltd, London (1961) p. 313.
[16] D. J. Pietrzyk and C. W. Frank, 'Analytical Chemistry', Academic Press, New York (1979) p. 557.
[17] S. Sathyanarayana, unpublished results.